

Ultrasonic Tinning of Al Busbars for a Silver-Free Rear Side on Bifacial Silicon Solar Cells

Malte Brinkmann^{ID}, *Graduate Student Member, IEEE*, Thomas Daschinger^{ID}, Rolf Brendel^{ID},
and Henning Schulte-Huxel^{ID}

Abstract—Reducing the silver consumption of photovoltaics (PV) is a major aspect in recent solar cell research. For bifacial PERC+ solar cells silver is used for the front contact. On the rear side aluminum metallization provides the contact to the silicon. The native oxide of aluminum prohibits a standard soldering process. Therefore, rear side silver pads are typically used for the cell-to-cell interconnections with copper wires. Silver can be avoided when using ultrasonic soldering for wetting the aluminum metallization to form tin solder pads. We demonstrate mechanically stable soldering of interconnects to the silver-free solder pads with a median adhesion up to 3 N/mm. We observe a penetration of the native aluminum oxide layer by the ultrasonic tinning process and the formation of metal-to-metal contacts from the aluminum to the solder. Resistance measurements demonstrate a reduced series resistance of the ultrasonically prepared contact when compared with using silver pads. For PERC+ cells, we can thus fully avoid rear side silver pads for a standard stringing process to reduce the silver consumption by 20%–40%. We fabricate mini modules that reach the same efficiency as reference modules with standard silver pads on the rear. The efficiency degradation of the modules with the ultrasonic interconnection is less than 3.6% after 200 humidity-freeze cycles and less than 2.2% after 600 temperature cycles.

Index Terms—Aluminum contacting, cell interconnection, lead-free, silver consumption, ultrasonic soldering.

I. INTRODUCTION

THE silver and lead consumption of the photovoltaic (PV) sector is a major concern towards the goal of a 100% renewable energy production [1], [2]. Silicon solar cells typically require silver for contacting the Si wafer and for the interconnection of the cells in a PV module. Bifacial passivated emitter and rear contact (PERC+) solar cells are presently the mainstream technology with the lowest Ag consumption [1]. It uses Ag fingers and busbars for the front contact and Ag pads for soldering on the rear side. The Al busbar on the rear of PERC+

Received 9 June 2024; revised 8 November 2024; accepted 15 January 2025. Date of publication 6 February 2025; date of current version 19 February 2025. This work was supported in part by the German Federal Ministry for Economic Affairs and Climate Action (BMWK) under Contact 03EE1080C (TOP) and in part by the State of Lower Saxony through the Artemis Project within the special fund for economic development, ecological area, Chapter 5157. (*Corresponding author*: Malte Brinkmann.)

Malte Brinkmann, Thomas Daschinger, and Henning Schulte-Huxel are with the Institute for Solar Energy Research Hamelin, 31860 Emmerthal, Germany (e-mail: brinkmann@isfh.de).

Rolf Brendel is with the Institute for Solar Energy Research Hamelin, 31860 Emmerthal, Germany, and also with the Institute for Solid State Physics, Leibniz University Hannover, 30167 Hannover, Germany.

Digital Object Identifier 10.1109/JPHOTOV.2025.3533901

cells cannot be contacted by standard soldering because of the stable native aluminum oxide. Thus, Ag pads are typically used for soldering [3].

Ultrasonic (US) soldering is a process for breaking up the aluminum oxide layer by generating cavities in molten solder. The solder is in contact with the oxidized aluminum metallization. The cavities implode, generating shock waves that impact on the Al oxide and thereby break up the oxide layer to achieve an intermetallic contact. After solidification of the solder, a solderable surface is generated [4].

In PV, US soldering can be used to tin aluminum to prepare silver-free tin pads. To avoid confusion with the standard soldering process of cell interconnects, the ultrasonic process to prepare tin pads on Al metallization will be referenced as US tinning. It is highly compatible with the standard stringing process using solder-coated copper wires. The Ag pad print is replaced by US tinning of aluminum. Hence, it does not increase the number of processing steps during cell production. US tinning was already investigated by ISFH in the early 2000s for the tinning of aluminum to prepare silver-free tin pads [5].

In addition, an obvious disadvantage of using Ag pads is avoided when using US tinning to form tin pads: The amount of costly Ag is reduced. Further, Ag and Al form a composite with a resistivity that can be 20 times higher than that of pure aluminum [6]. Tin-aluminum alloys have a more than six times lower resistivity than the silver-aluminum alloy [7] thus enabling a reduction in series resistance when using ultrasonic tinning.

In the last 15 years, US tinning was applied for the production of silver-free solder pads to string solar cells having a rear side with a full area metallization [8], [9], [10]. However, the peel forces barely exceeded the required 1 N/mm as stipulated by standard DIN EN 50461 [10].

Applying US tinning to bifacial PERC+ cells with busbars raises additional challenges. Narrow busbars with a width of only a few millimetres or less are more demanding for achieving mechanical stability and low electrical resistivity with US tinning. To the best of our knowledge, US tinning has not been applied to bifacial solar cells that have fingers and busbars made of aluminum.

In this article, we investigate and demonstrate US tinning of Al busbars on the rear side of PERC+ cells. We fabricate mini modules with this US mediated interconnection technique. Our process wets the aluminum metallization with tin or tin composites and thus enables Ag-free solder pads. Potential induced damage of the US tinning process on the cell is tested

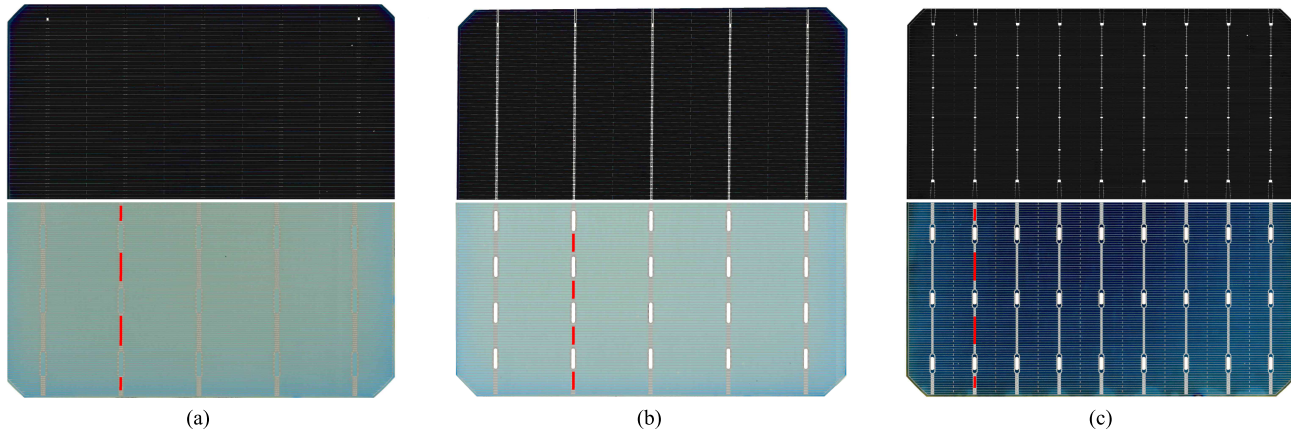


Fig. 1. Front and rear side of the PERC+ solar cells used in this article. Cell type A is a cell with a 5BB metal grid layout without an Ag front busbar and rear Ag pad print. Cell type B has a 5BB print and cell type C has a 9BB layout. B and C have a standard metallization on both sides. The red lines indicate the tinned areas, exemplarily shown on the second to left busbar on each cell.

via photoluminescence (PL) imaging as well as current-voltage (*I*-*V*) measurements. We investigate the US tinned contacts by scanning electron microscopy and measure the mechanical stability as well as the contact resistance of the interconnects to the cell. We present mini modules with a rear side connection using ultrasonically prepared tin pads and their aging behavior under thermal cycling and humidity-freeze (HF) cycles. For all experiments, lead-free solders are used showing the applicability for lead-free PV modules.

II. ULTRASONIC TINNING PROCESS

The US tinning process is applied to three different industrial PERC+ solar cells. Fig. 1 shows the front and the rear side of the cells and their metal grid layout. Two have a 5 busbar (5BB) layout (cell type A and B) and one has a 9 busbar (9BB) layout (cell type C). Cell type A and B both have a M2 wafer size and were produced in 2020. The width of the Al busbars on the rear side of these cells is 2 mm. Cell type C has a M6 wafer size, was produced in 2023, and has an Al busbar width of 1 mm. The red lines in Fig. 1 indicate the position of areas which are tinned during the ultrasonic process. They have a width of 1 mm and are between 5 and 12 mm long, depending on the available space between two Ag pads. We present the US tinning on these two generations of PERC+ solar cells that were fabricated by two different top ten solar cell manufacturing companies. The intention is to demonstrate that the process is not limited to a specific cell type.

The ultrasonic tinning is performed with an US soldering station by MBR Electronics using a sonotrode with a diameter of 1 mm. The US frequency is 60 kHz. The station allows an US power range from 4 W to 12 W with an adjustable temperature of the solder iron tip from 150 °C to 480 °C. The tinning material is a lead-free Sn90Zn10 composite. Zinc improves the US-assisted contact formation to aluminum [11] and reduces the melting point of 232 °C for pure tin to 199 °C of the composite.

The Al busbar on the rear side in between two Ag solder pads or an Ag pad and the cell edge is tinned to prepare US tin pads. The US sonotrode collects the solder from a solder bath heated

to 220 °C. The low heating power of the solder tip requires a heating of the solar cell to 180 °C during the process to prevent solidification of the solder during application. The US tinning provides silver-free solderable areas on the Al busbars. We use a manual soldering process with a handheld solder iron to solder copper ribbons to these tinned areas. The ribbons have a cross section of 1.3 mm × 0.2 mm. They are coated with Sn96.5Ag3.5 lead-free solder.

It is required to block the Ag pads on the rear side of cell types B and C for testing the mechanical adhesion as well as for the fabrication of mini modules. Therefore, we tape a 70 µm thick adhesive polyimide film over the Ag solder pads on the cells to prevent soldering to the Ag pads and ensure a connection to the tin pads only.

III. RESULTS

A. Damage Inspection

During the US tinning process on the rear side Al busbars sound waves are coupled into the solar cell metallization that could possibly damage the surface passivation and enhance the recombination of light-generated carriers. PL imaging monitors potential damage on the solar cell. Cell type A without Ag busbar allows examination of the areas below the rear side busbars. The PL images in Fig. 2 show the front side of a 5 BB solar cell of cell type A (see Fig. 1) before and after US assisted wetting of the rear side busbars with the maximum achievable US power of 12 W and 300 °C of the US solder iron tip. The reduction in luminescence is less than 1% under the tinned areas. Applying ultrasonic power to a nonmetallized area induces severe damage in the solar cell, presumably because of damage on the passivation layers. Nevertheless, even a busbar width of 2 mm is easy to handle with the manual process. Two different operators tinned more than 20 cells each with no damage to the solar cell.

9BB cells without an Ag busbar print were not available. Therefore, damage inspection via PL imaging is not possible because of the Ag busbar on the front side. We measure the *I*-*V* characteristics with a LOANA system to detect any induced

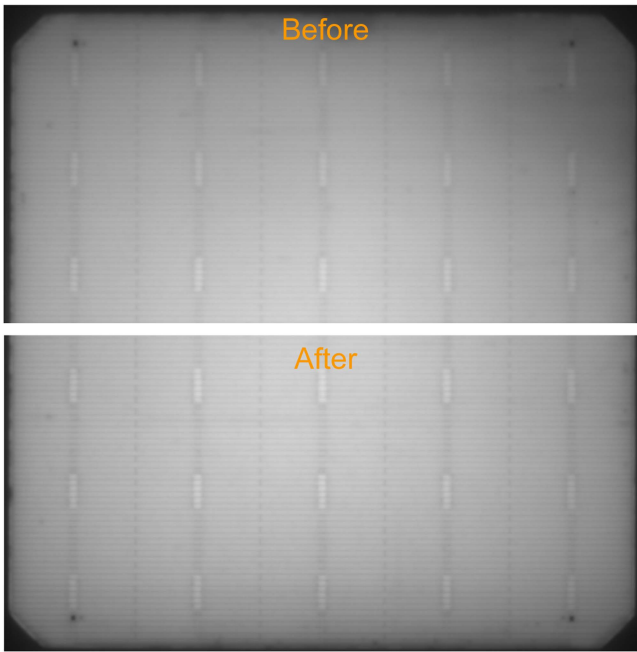


Fig. 2. PL image of the front side of an Ag busbar-free solar cell type A before (top) and after (bottom) US tinning of Al busbars on rear side with an US power of 12 W.

damage. The reduction in open circuit voltage V_{OC} is below the measurement uncertainty of 0.2% and the efficiency loss is below the measurement uncertainty of 0.2 %_{rel}.

B. Mechanical Adhesion

According to standard DIN EN 50461 the minimal pull force cell interconnects must withstand is 1 N per millimetre connector width. A force-path tool measures the peel forces of interconnects soldered to US tin pads in 180° pull testing. Each interconnect is soldered to seven to eight US tin pads per busbar, depending on the metallization layout of the full cell. We measure the peel force for the full interconnect as a function of distance. There is no adhesion between two pads, therefore they can be easily separated in the path-force graphs. For each pad, the maximum of the measured force is derived to determine the peak pull force. We measure the adhesion on cells of cell type A (see Fig. 1) for different parameters of the US tinning process. The ultrasonic tinning of the Al busbar between two pad positions uses US tinning powers ranging from 4 to 12 W in 2 W steps and US solder iron temperatures of 250 °C, 300 °C, and 400 °C. We solder copper interconnects to the tinned areas. They have more than twice the length of the cell. Fig. 3(a) shows the forces required to peel of the interconnect of the US tin pads. The adhesion of the copper interconnects increases with the ultrasonic power up to 10 W. Temperatures of 300 °C and 400 °C are favorable in contrast with the lower temperature of 250 °C. The pull force for US powers of more than 10 W and temperatures of 300 °C and 400 °C exceeds the required value of 1 N/mm with a median peel force of 1.5 N/mm to 2.8 N/mm.

Additionally, we test the influence of the movement speed of the US sonotrode on the cell during the tinning process on

9BB cells of cell type C. A robot arm moves the US soldering head with velocity in the range of 25–250 mm/s. The mechanical adhesion is tested for 6 W and 10 W at a sonotrode temperature of 300 °C. The median pull force shown in Fig. 3(b) slightly increases for higher velocities for both 6 and 10 W of ultrasonic power reaching a median of up to 3 N/mm for 10 W. The 9BB cells show improved adhesion of the interconnects as higher peel forces are achieved for all parameters compared with the 5BB cell.

One explanation of the improved mechanical adhesion compared with previously published values on full-area screen printed cells in [10] could be the advancement of the Al pastes. The composition of the pastes changes after firing in case of a finger structure compared with a full area metallization [12]. This results in an improved contact of the Al fingers and busbars to the silicon bulk of the solar cell.

A closer examination of the fracture location reveals that for 95% of the contacts that, the breaking point occurs in the Al busbar paste which is ripped off the cell surface together with the interconnects. For roughly 5% of contacts the tin pad is peeled off from the busbar. We conclude that the US tinned connection is predominantly limited by the adhesion of the Al paste to the wafer surface and not by the soldered cell interconnects to the US tin pads.

The solder spots with low adhesion are mainly the outermost ones at the beginning and end of the busbars. The interconnects are heated above the melting point of the SnAg solder of 221 °C during soldering. As the pull force experiments were performed on full cells the cooled down cells exhibit high mechanical stress because of the different thermal expansion of the copper interconnects and the silicon solar cell. This stress has the highest impact on the edge of the solar cell leading to partial peel-off of the interconnects before the actual experiment. This can be relaxed by a half-cell design as it is the standard for PV modules and the mini modules presented in Section VI.

Moving speed of up to 250 mm/s of the US soldering head achieves a reliable mechanical contact and thus allows a process time of below one second per busbar. Using the same number US soldering irons as the number of busbars enables a process time below one second per cell. Such process times are compatible with current production lines.

US tinning parameters of 300 °C and 10 W have shown robust and mechanically stable connections. Thus, the US process is applied with these parameters for the experiments presented in Section V and VI.

IV. STRUCTURAL ANALYSIS

We analyse the ultrasonically tinned busbars with scanning electron microscopy. The US tinning is applied to Al busbars of cell type C with ultrasonic power of 4 W and 10 W at 300 °C. Images of cross sections shown in Fig. 4(a) and (b) indicate the formation of a layer of solder on top of the busbar with a thickness of about 10 μm. The solder penetrates the Al metallization filling the holes between the Al spheres of the paste. The penetration depth depends on the US power. For 4 W, the solder accumulates only in the top half of the busbar explaining the

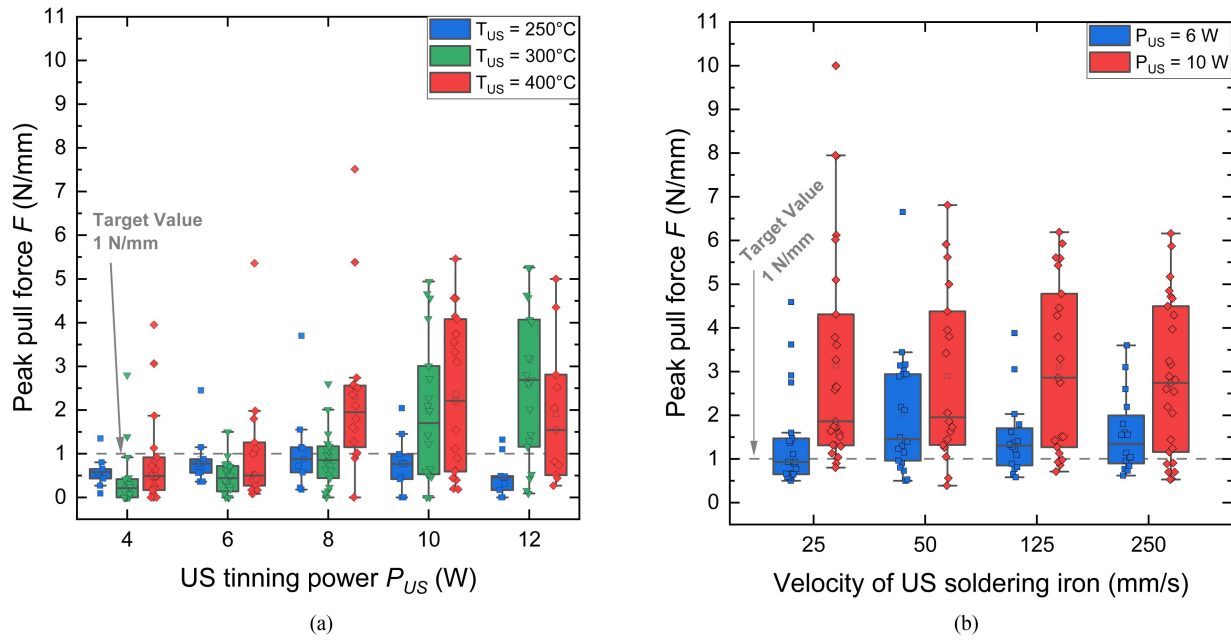


Fig. 3. Maximum pull force required to peel cell interconnect from ultrasonically tinned solder pad for various US powers P_{US} and temperatures T_{US} of the sonotrode on cell type A (a) and for different US powers P_{US} and moving speeds of the US solder iron on cells of type C (b).

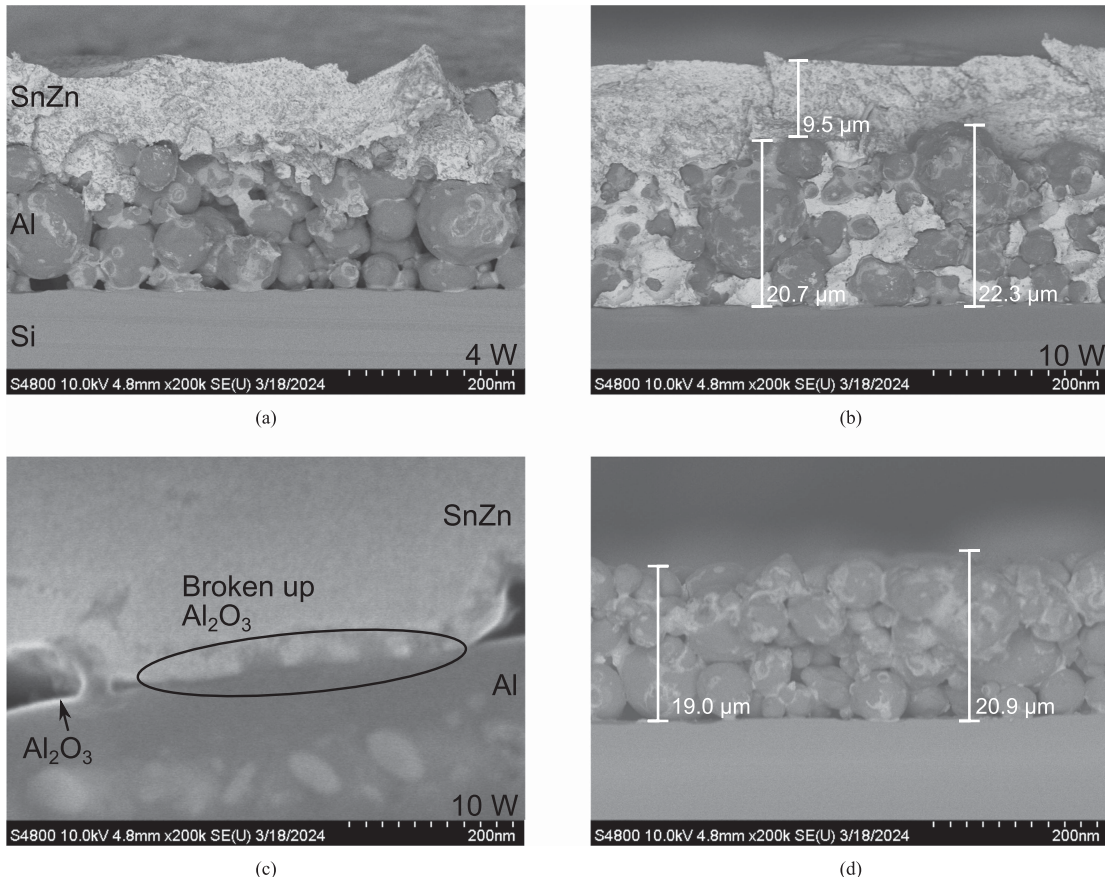


Fig. 4. Cross section SEM images of ultrasonically tinned busbars with ultrasonic powers of (a) 4 W and (b) 10 W. The light gray material is the solder, the dark gray spheres correspond to the Al paste. Subfigure (c) shows a cross section polished via ion beam etching cutting through the solder and the sphere showing the metal to metal contact. In (d) an unmodified busbar is shown as reference.

TABLE I
LINE RESISTANCE OF BUSBAR BEFORE AND AFTER US TINNING FOR DIFFERENT US POWERS P_{US} MEASURED WITH A FOUR-POINT PROBE

P_{US} [W]	Line resistance [mΩ/cm]
4	30.0 ± 1.8
7	27.2 ± 1.4
10	24.8 ± 1.4
Pure Al busbar	40.2 ± 1.6

limited adhesion of the cell interconnects shown in the previous section. Using an US Power of 10 W results in a full penetration of the busbar by the solder down to the silicon wafer resulting in a good mechanical stability of the connection.

A cross section of a busbar tinned with US power of 10 W is polished with an ion milling system. This allows cutting through the solder and Al spheres to inspect the contact formation. Fig. 4(c) shows a strongly magnified picture of the contact. We observe the breaking of the Al_2O_3 layer and a direct contact of the solder and the aluminum in the highlighted area. Additionally, aluminum migrates in the solder which can be seen by the dark areas fading out into the lighter sphere of the solder at the interface. This proves the penetration of the native aluminum oxide layer on the Al via the ultrasonic soldering process. The ultrasonic tinning process not only pushes the solder into the voids in the Al paste but also creates intermetallic contacts.

Comparing the soldered busbars to an unmodified busbar in Fig. 4(d) reveals no densification or removal of the Al metallization because of the US soldering process for both 4 W and 10 W. The height and position of the Al particles are preserved with an overall height of the busbar of ca. $20 \mu\text{m}$ before and after US tinning. Thus, we expect only a minimal accumulation of paste residues on the US soldering tips and no enhanced requirements on the cleaning of the tips in a production line.

V. ELECTRICAL PERFORMANCE

The electrical properties of the US contact have an influence on the series resistance of the PV module. We test the impact of the US tinning on the line resistance of the busbar. We measure the resistance before and after US tinning at 4 W, 7 W, and 10 W using four-point probe measurement configuration. The application of the tinning process reduces the line resistance of the busbar up to 40% for an US Power P_{US} of 10 W as shown in Table I. Additionally, we prepare a similar line of solder on a glass substrate to measure the resistance of the applied solder during the process. The amount of solder added to the busbar and in the line on glass is comparable. The resistance of the solder on glass is an order of magnitude higher with $300 \pm 30 \text{ m}\Omega/\text{cm}$. Therefore, the resistance is not dominated by the additional amount of solder. The positive impact on the line resistance originates from the void filling in the Al metallization and the metal-to-metal connection of solder and aluminum demonstrating an additional positive impact of the ultrasonic tinning.

Additionally, we analyze the contact resistance of US tinned contact and compare it to the resistance of the contact with silver pads. For a full comparison of its impact on the series resistance

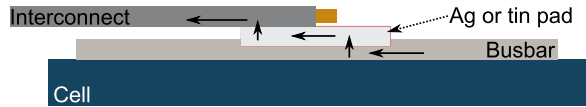


Fig. 5. Schematic cross-sectional view of contact area (not to scale). The arrows depict the measured path resistance.

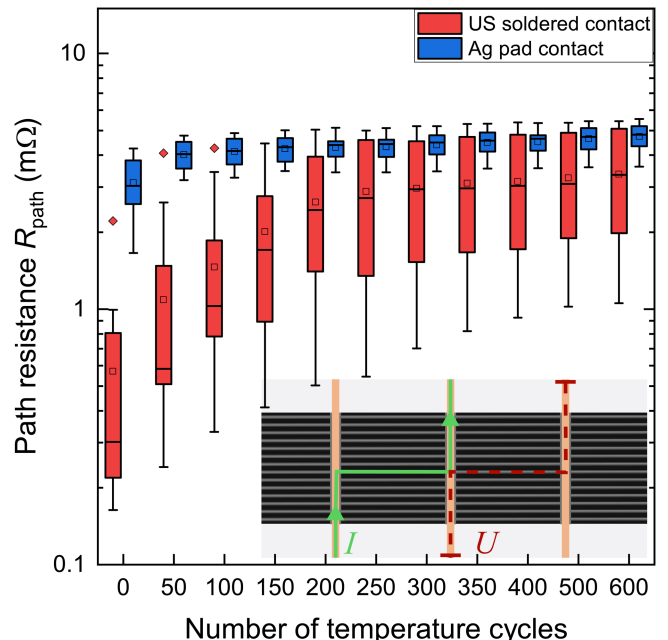


Fig. 6. Ageing behavior of path resistance from Al busbar to copper interconnect via US tinned solder pad and Ag solder pad, respectively. The inset shows the schematic of the measurement configuration (not to scale) with the measured voltage (red) and current path (green).

of the solar cell, the resistance of the Al/Ag and Al/SnZn interfaces needs to be considered. Therefore, we measure the path resistance R_{path} from an aluminum busbar to a cell interconnect for both the ultrasonically produced solder pads and standard Ag solder pads. Fig. 5 shows the measurement path.

Test modules are prepared with 1 cm thin cell stripes cut perpendicular to busbars. Cell interconnects are soldered to each busbar either via US tin pads or standard Ag solder pads. We ensure that the US tinned pads have approximately the same size as the Ag pads of $1 \text{ mm} \times 5 \text{ mm}$ for a direct comparison. The principle of the resistance measurement is depicted in the inset of Fig. 6, showing the induced current path from one interconnect to the next. This emulates the current path in the cell metallization from finger to busbar. The voltage is measured over the next pair of interconnects resulting in an effective resistance measurement from the Al busbar to the interconnect via the US tinned or Ag pad of the middle contact.

The ultrasonically applied tin pads initially perform better with a median path resistance of $0.3 \text{ m}\Omega$ compared with the Ag solder pads with a path resistance of $3 \text{ m}\Omega$ (see Fig. 6). The high resistivity of the Al/Ag composite formed at the overlap of the solder pad and the busbar limits the path resistance of the conventional contact. The lower resistance of the US contact improves the fill factor of the cell by 0.1%. The manual process leads to small deviations in width and length of the ultrasonically

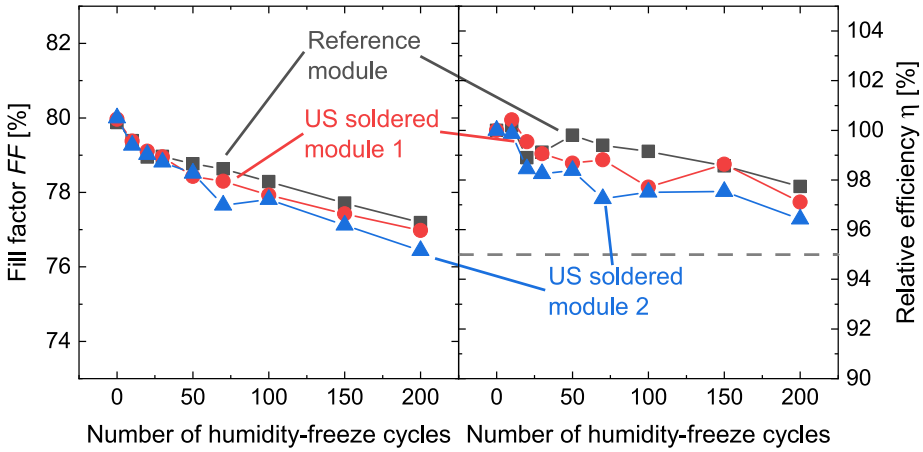


Fig. 7. Ageing behavior of modules containing 1 half-cut cell of type B under HF cycling. The efficiency and fill factor of two modules with an US contact (red, blue) are compared with a reference module with standard Ag contacting (black). The gray dashed line shows the maximum allowed efficiency degradation of 5%_{rel}.

TABLE II

I–V CHARACTERISTICS OF FABRICATED MODULES USING US TINNING PROCESS; THE MODULES ARE MEASURED IN A MODULE FLASHER WITH RELATIVE UNCERTAINTIES OF 0.2% IN V_{OC} , 0.1% J_{SC} , AND 0.5% IN FILL FACTOR AND EFFICIENCY

	V_{OC} [V]	J_{SC} [mA/cm^2]	Fill factor [%]	Efficiency [%]
US Module 1	0.640	36.61	79.96	18.73
US Module 2	0.644	36.63	79.99	18.87
Reference module 1	0.640	36.47	79.87	18.57
US Module 3	3.45	36.96	80.67	20.63
Reference module 2	3.46	36.83	80.61	20.49

applied solder pads. Thus, the measured values for the ultrasonic connection have a higher span because of variations of the effective contacting area.

The test modules are exposed to thermal cycling (TC) from -40°C to 85°C for accelerated ageing testing of the contacts. The Ag contacts are more stable under ageing and have a smaller relative increase to $4.5 \text{ m}\Omega$ after 600 TC cycles. The path resistance of the tinned contact shows a larger increase in path resistance which is, however, still lower with $2.5 \text{ m}\Omega$ after ageing.

Using the US tinning process also enables a larger contacting area. Adapting the grid design to continuous busbars would allow US tinning of a large fraction of the busbar and thus a bigger contact area reducing the resistance even further.

VI. MODULE PERFORMANCE

We test the performance and the ageing stability of the US tinned contact by preparing several mini modules. All modules are glass-backsheet modules with Polyolefin Elastomers as encapsulant. Three of the mini modules contain one half-cut 5BB cell (cell type B, see Fig. 1) each. Two of these are produced with a rear side contacting via ultrasonic tin pads (US modules

1 & 2). One module with Ag pad contacting on the rear side is fabricated as a reference (Reference module 1). The modules are measured with a module flasher. The initial *I–V* parameters are shown in Table II. The US modules show slightly improved performance with 0.1% higher fill factors and 0.15%–0.3% higher efficiencies. This coincides with the reduced resistance of the contact presented in Section V.

The mini modules are exposed to HF cycling ranging from $85^\circ\text{C}/85\%$ rel. humidity to -40°C . The ageing behavior of the fill factor and efficiency is shown in Fig. 7. The fill factor of all modules degrades similarly with finger interruptions being the main degradation process resulting in varying absolute fill factor losses. This is the reason for the slightly increased fill factor and efficiency losses of US module 1 and 2 compared with the reference module. The increased ageing of the path resistance of the US contact presented in Section V results in an expected increased fill factor degradation of 0.1%_{rel} compared with the reference module.

After 200 HF cycles, exceeding the required ten cycles of standard IEC 61215, the loss in efficiency is less than 3.6%_{rel} for the two modules with ultrasonic tinning and thus below the maximum allowed efficiency degradation of 5%_{rel}.

Two additional mini modules were fabricated for accelerated ageing with thermal cycling. The modules contain one string of five half-cut 9BB cells each (cell type C, see Fig. 1). The cell gap is 3 mm. One module is prepared with ultrasonic tinned pads on the rear side (US module 3) and one module has the standard Ag pad contacting (Reference module 2). Fig. 8 shows an electroluminescence image of the US module 3. The fabrication introduces two small cracks, which we assign to the manual soldering of interconnects as it is more susceptible to cell breakage. Contacting the solar cell close to the edge is challenging using commercial solar cells with a standard print. It is required to contact the busbar between the cell edge and the outermost Ag solder pads for a sufficient electrical contact. The limited area and working so close to the edge introduce a high risk of cell breakage or failed contacts [13], [14], which can be seen by the dark area on the second cell from the right

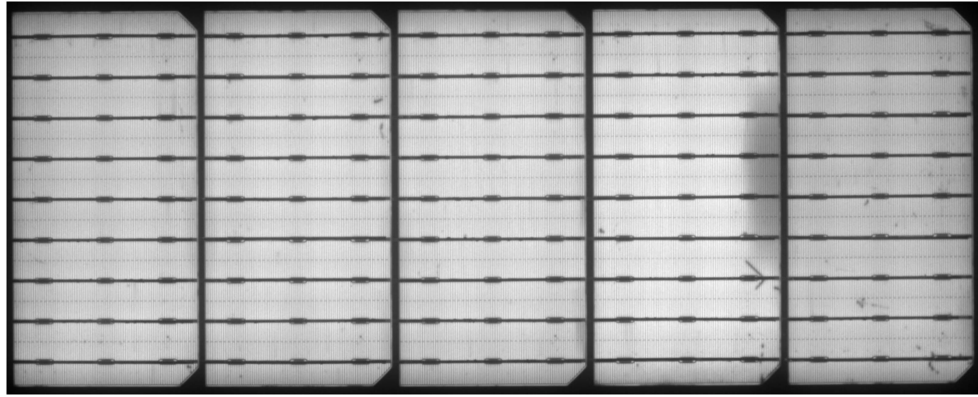


Fig. 8. EL image of the rear side of mini module *US Module 3* containing five half-cut cells with ultrasonically prepared solder pads on the rear side.

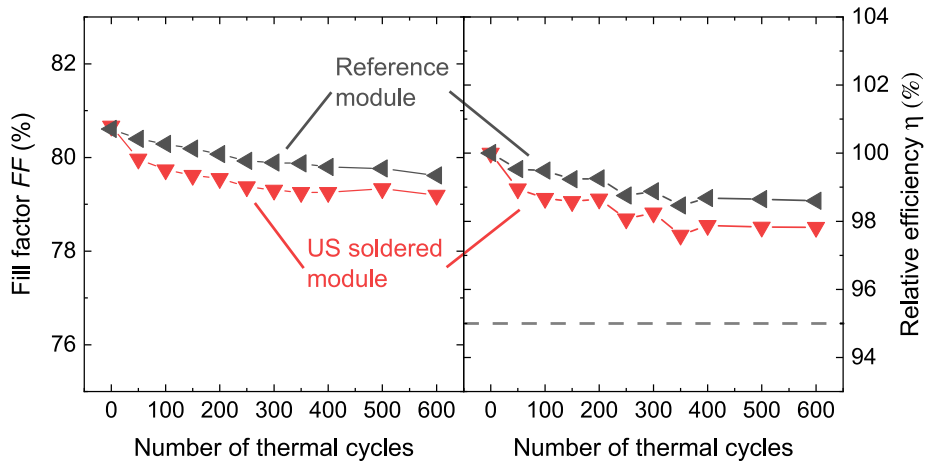


Fig. 9. Ageing behavior of fill factor and efficiency of mini module containing a string of 5 type C cells under temperature cycling. A module with an US contact (red) is compared with a reference module with standard Ag contact (black). The gray dashed line shows the maximum allowed efficiency degradation of 5%_{rel}.

in Fig. 8. Using a continuous busbar design would relax this problem drastically as the ultrasonic tin pads do not have to be so close to the cell edge. Such cells were not available at that time.

Nevertheless, the initial fill factor and efficiency are slightly improved, as shown in Table II. The ageing behavior of the modules of up to 600 TC cycles is presented in Fig. 9. The reference module degrades less than the US module. The higher losses in fill factor of the US module are a result from the nonideal layout of the metal grid on the rear side as described before. After the required 600 temperature cycles of standard IEC 61215 the module efficiency is only reduced by 2.2% well below the maximum allowed degradation of 5%.

VII. CONCLUSION

We demonstrate an almost silver-free and lead-free interconnection on the rear side of bifacial PERC+ solar cells using an ultrasonic assisted soldering. The US process is used to tin Al busbars and prepare solderable and silver-free areas on top of the busbar. The damage-free process improves the electrical path resistance from Al metallization to copper ribbon by a factor

of two after accelerated ageing. The mechanical adhesion of up to 3 N/mm exceeds the peel force of previously published values for full area screen-printed solar cells [10] by more than a factor of two. Mini modules with US contacting show similar *I*-*V* characteristics to those with silver contacts. They withstand 200 HF cycles with efficiency losses below 3.6% and 600 temperature cycles with a degradation of less than 2.2% in module efficiency.

The rear side Ag pads of bifacial PERC+ require 20–40 mg per cell [15]. Using US tinning to contact Al busbars offers a reduced silver consumption such solar cell by 15%–30% [15]. Omitting the rear side Ag pads also enables improved module efficiency if the metal grid is adapted. The contact area can be increased by US tinning of the whole busbar decreasing the series resistance even further. Additionally, the elongated current path for majority charge carriers in the bulk above the rear side Ag pads is eliminated reducing the series resistance of the module [16]. Furthermore, the recombination that is typically induced by the Ag pads is avoided when using US tinning [16], [17]. Using a Al metal grid without Ag pads on the rear side can increase module efficiencies by 0.1 %_{abs} to 0.2_{abs} [16].

The consumption of lead in PV module production plays a critical role for sustainable and eco-friendly modules. The major fraction of lead is introduced in the modules from the solder of the cell interconnects [2]. The process that we present in this article generates fully lead-free rear side cell interconnections.

VIII. OUTLOOK

The work presented in this article is the basis for the silver-free cell interconnection of high-efficiency cell concepts with an aluminum metallization. For example, the POLO back junction cell is realized with the p-contact on the illuminated side requiring an aluminum metal grid on the front [18]. Currently, silver pads would be necessary for the cell interconnection. To avoid high shading losses the size of the Ag pads and thus the overlap of the Al busbar and Ag pads is limited. This results in high resistivities on the scale of $300\text{ m}\Omega$ from Al busbar to Ag pad [19]. Using US tinning not only reduces the silver consumption. It also enables larger contact areas by tinning the whole busbar for a lower contact resistance without increased shading losses. The POLO-BJ cell concept has also been realized with aluminum for both contacts [20]. Therefore, the US tinning technique enables the interconnection of high-efficiency and silver-free Si solar cells.

Ultrasonic tinning enables silver-free interconnection of other cell types and concepts using an Al metal grid. For example, TOPCon solar cells have been realized with aluminum contacts as well [21]. US tinning can also be adapted to back contact solar cells with Al metallization like the record-breaking POLO-IBC cell developed at our Institute for Solar Energy Research in Hamelin [22] or p-type hybrid passivated back contact cells (HPBC).

ACKNOWLEDGMENT

The authors would like to thank M. Köntges for fruitful discussion and input. The authors would also like to thank I. Kunze, R. Delsol, and S. Bräunig for their help toward the presented results, R. Clausing for proof-reading as well as J. Schoenbür and S. Blankemeyer from the *match* institute of the Leibniz University Hannover for their support on the experiments with the robotic handling of the US solder iron.

REFERENCES

- [1] Y. Zhang, M. Kim, L. Wang, P. Verlinden, and B. Hallam, "Design considerations for multi-terawatt scale manufacturing of existing and future photovoltaic technologies: Challenges and opportunities related to silver, indium and bismuth consumption," *Energy Environ. Sci.*, vol. 14, no. 11, pp. 5587–5610, 2021, doi: [10.1039/D1EE01814K](https://doi.org/10.1039/D1EE01814K).
- [2] O. Malandrino, D. Sica, M. Testa, and S. Supino, "Policies and measures for sustainable management of solar panel end-of-life in Italy," *Sustainability*, vol. 9, no. 5, 2017, Art. no. 481, doi: [10.3390/su9040481](https://doi.org/10.3390/su9040481).
- [3] T. Urban, M. Heimann, A. Schmid, A. Mette, and J. Heitmann, "Analysis of ohmic losses due to solder and pressure interconnection and related interface resistances for solar cells," *Energy Procedia*, vol. 77, pp. 420–427, 2015, doi: [10.1016/j.egypro.2015.07.059](https://doi.org/10.1016/j.egypro.2015.07.059).
- [4] K. Graff, "Macrosonics in industry: Ultrasonic soldering," *Ultrasonics*, vol. 15, no. 2, pp. 75–81, doi: [10.1016/0041-624X\(77\)90069-5](https://doi.org/10.1016/0041-624X(77)90069-5).
- [5] M. Köntges and I. Kunze, "Final internal report of FZS project funded by Federal Ministry for the Environment, Nature Conservation and Nuclear Safety, FKZ: 0329717 C, Institut für Solarenergie Forschung Hameln," 2005.
- [6] J. J. van den Broek, A. G. Dirks, and P. E. Wierenga, "The composition dependence of internal stress, ultramicrohardness and electrical resistivity of binary alloy films containing silver, aluminium, gold, cobalt, copper, iron or nickel," *Thin Solid Films*, vol. 130, no. 1–2, pp. 95–101, 1985, doi: [10.1016/0040-6090\(85\)90299-8](https://doi.org/10.1016/0040-6090(85)90299-8).
- [7] F. M. Tezel, B. Saatci, M. Ari, S. Durmus Acer, and E. Altuner, "Structural and thermo-electrical properties of Sn-Al alloys," *Appl. Phys. A*, vol. 122, no. 10, pp. 1–12, 2016, doi: [10.1007/s00339-016-0398-8](https://doi.org/10.1007/s00339-016-0398-8).
- [8] H. von Campe, S. Huber, S. Meyer, S. Reiff, and J. Vietor, "Direct tin-coating of the aluminum rear contact by ultrasonic soldering," in *Proc. 27th Eur. Photovoltaic Sol. Energy Conf. Exhib.*, 2012, pp. 1150–1153, doi: [10.4229/27theUPVSEC2012-2AV.5.32](https://doi.org/10.4229/27theUPVSEC2012-2AV.5.32).
- [9] H. Nagel, D. Eberlein, S. Hoffmann, M. Graf, and T. Buck, "Ultrasonically tinned PVD Al rear contacts on high-efficiency crystalline silicon solar cells for module integration," in *Proc. 37th Eur. Photovolt. Sol. Energy Conf. Exhib.*, 2017, pp. 295–299, doi: [10.4229/EUPVSEC20172017-2AO.6.5](https://doi.org/10.4229/EUPVSEC20172017-2AO.6.5).
- [10] P. Schmitt et al., "Adhesion of Al-metallization in ultra-sonic soldering on the Al-rear side of solar cells," *Energy Procedia*, vol. 38, pp. 380–386, 2013, doi: [10.1016/j.egypro.2013.07.293](https://doi.org/10.1016/j.egypro.2013.07.293).
- [11] W. Guo, T. Luan, J. He, and J. Yan, "Ultrasonic-assisted soldering of fine-grained 7034 aluminum alloy using Sn-Zn solders below 300 °C," *Ultrasonics Sonochemistry*, vol. 40, no. Pt A., pp. 815–821, 2018, doi: [10.1016/j.ultsonch.2017.08.020](https://doi.org/10.1016/j.ultsonch.2017.08.020).
- [12] C. Kranz, B. Wolpensinger, R. Brendel, and T. Dullweber, "Analysis of local aluminum rear contacts of bifacial PERC solar cells," *IEEE J. Photovolt.*, vol. 6, no. 4, pp. 830–836, Apr. 2016, doi: [10.1109/JPHOTOV.2016.2551465](https://doi.org/10.1109/JPHOTOV.2016.2551465).
- [13] S. Dietrich, M. Pander, M. Sander, and M. Ebert, "Mechanical investigations on metallization layouts of solar cells with respect to module reliability," *Energy Procedia*, vol. 38, pp. 488–497, 2013, doi: [10.1016/j.egypro.2013.07.308](https://doi.org/10.1016/j.egypro.2013.07.308).
- [14] L. C. Rendler et al., "Thermomechanical stress in solar cells: Contact pad modeling and reliability analysis," *Sol. Energy Mater. Sol. Cells*, vol. 196, pp. 167–177, 2019, doi: [10.1016/j.solmat.2019.03.041](https://doi.org/10.1016/j.solmat.2019.03.041).
- [15] S. K. Chunduri and M. Schmela, "Market survey—metallization pastes 2019/2020," Taiyang News, 2020.
- [16] H. Schulte-Huxel et al., "Impact of Ag pads on the series resistance of PERC solar cells," *Energy Procedia*, vol. 92, pp. 743–749, 2016, doi: [10.1016/j.egypro.2016.07.053](https://doi.org/10.1016/j.egypro.2016.07.053).
- [17] T. Urban, A. Mette, and J. Heitmann, "Influence of silver-aluminium alloy at solar cell rear side on series resistance and open circuit voltage," *Energy Procedia*, vol. 92, pp. 236–241, 2016, doi: [10.1016/j.egypro.2016.07.065](https://doi.org/10.1016/j.egypro.2016.07.065).
- [18] R. Peibst et al., "On the chances and challenges of combining electron-collecting *n*POLO and hole-collecting Al-*p*⁺ contacts in highly efficient *p*-type c-Si solar cells," *Progr. Photovoltaics: Res. Appl.*, vol. 31, no. 4, pp. 327–340, 2023, doi: [10.1002/pip.3545](https://doi.org/10.1002/pip.3545).
- [19] H. Schulte-Huxel, T. Daschinger, B. Min, T. Brendemühl, and R. Brendel, "Novel busbar design for screen-printed front side Al metallization of high-efficiency solar cell," *Sol. Energy Mater. Sol. Cells*, vol. 264, 2014, Art. no. 112601, doi: [10.1016/j.solmat.2023.112601](https://doi.org/10.1016/j.solmat.2023.112601).
- [20] B. Min et al., "All-aluminum screen-printed POLO back junction solar cells," in *Proc. 40th Eur. Photovolt. Sol. Energy Conf. Exhib.*, 2023, pp. 020044-001–020044-004, doi: [10.4229/EUPVSEC2023/ICV.3.2](https://doi.org/10.4229/EUPVSEC2023/ICV.3.2).
- [21] D. Ourinson et al., "Paste-based silver reduction for iTOPCon rear side metallization," *Sol. Energy Mater. Sol. Cells*, vol. 266, 2024, Art. no. 122646, doi: [10.1016/j.solmat.2023.112646](https://doi.org/10.1016/j.solmat.2023.112646).
- [22] F. Haase et al., "Laser contact openings for local poly-Si-metal contacts enabling 26.1%-efficient POLO-IBC solar cells," *Sol. Energy Mater. Sol. Cells*, vol. 186, pp. 184–193, 2018, doi: [10.1016/j.solmat.2018.06.020](https://doi.org/10.1016/j.solmat.2018.06.020).